EFFECTIVE PHOSPHATE REMOVAL FROM AQUEOUS SOLUTIONS BY ELECTROCOAGULATION WITH ALUMINUM ELECTRODES AND POLARITY REVERSAL MODE

Nguyen Trong Nghia
Hung Yen University of Technology and Education

ARTICLE INFO

Received: 20/4/2025
Revised: 21/5/2025
Published: 22/5/2025

KEYWORDS

Optimization
Phosphate removal
Electrocoagulation
Polarity reversal mode
Aluminum electrode

ABSTRACT

Phosphate contamination in wastewater is a leading cause of eutrophication, posing serious threats to aquatic ecosystems and water quality. Mitigating this environmental issue requires the implementation of effective and sustainable treatment technologies. This study explores the application of a polarity reversal electrocoagulation system using aluminum electrodes for the efficient removal of phosphate from wastewater. Process parameters were systematically optimized using response surface methodology, with a central composite design employed to evaluate the interactive effects of current density, electrolysis time, and polarity reversal interval on phosphate removal efficiency. Phosphate percentage removal was selected as the response variable. The experimental data exhibited a strong fit with a quadratic model, indicating the significance of the selected operational parameters. Numerical optimization revealed that the highest phosphate removal was achieved under optimal conditions: current density of 46.8 A/m², electrolysis time of 50 minutes, and polarity reversal interval of 2.26 minutes. These findings demonstrate the potential of the polarity reversal electrocoagulation system as an effective and controllable approach for phosphate removal, offering practical implications for advanced wastewater treatment applications.

LOẠI BỎ PHỐT PHÁT HIỆU QUẢ TỪ DUNG DỊCH NƯỚC BẰNG PHƯƠNG PHÁP KEO TỤ ĐIỆN VỚI ĐIỆN CỰC NHÔM VÀ CHẾ ĐỘ ĐẢO NGƯỢC ĐIỆN CỰC

Nguyễn Trọng Nghĩa
Trường Đại học Sư phạm Kỹ thuật Hưng Yên

THÔNG TIN BÀI BÁO

Ngày nhận bài: 20/4/2025
Ngày hoàn thiện: 21/5/2025
Ngày đăng: 22/5/2025

TỪ KHÓA

Tối ưu hóa
Loại bỏ phốt phát
Keo tụ điện hóa
Chế độ đảo ngược điện cực
Điện cực nhôm

TÓM TẮT

Ô nhiễm phốt phát trong nước thải là nguyên nhân chính gây phú dưỡng, gây ra mối đe dọa nghiêm trọng đến hệ sinh thái dưới nước và chất lượng nước. Để giảm thiểu vấn đề môi trường này, cần phải triển khai các công nghệ xử lý hiệu quả và bền vững. Nghiên cứu này khám phá ứng dụng của hệ thống keo tụ điện hoá đảo cực sử dụng điện cực nhôm để loại bỏ hiệu quả phốt phát khỏi nước thải. Các thông số quy trình được tối ưu hóa một cách có hệ thống bằng phương pháp bề mặt đáp ứng với thiết kế tổng hợp trung tâm được sử dụng để đánh giá các tác động tương tác của mật độ dòng điện, thời gian điện phân và khoảng thời gian đảo cực đối với hiệu quả loại bỏ phốt phát. Tỷ lệ loại bỏ phốt phát được chọn làm biến phản hồi. Dữ liệu thực nghiệm cho thấy sự phù hợp chặt chẽ với mô hình bậc hai, chứng tỏ tầm quan trọng của các thông số vận hành đã chọn. Dựa trên kết quả tối ưu hóa số, tỉ lệ loại bỏ phốt phát đạt được giá trị cao nhất ở các điều kiện tối gồm: mật độ dòng điện bằng 46,8 A/m², thời gian điện phân trong 50 phút và thời gian đảo cực là 2,26 phút. Kết quả của nghiên cứu này chứng minh tiềm năng của hệ thống keo tụ điện hoá đảo cực như một phương pháp hiệu quả và có thể kiểm soát được để loại bỏ phốt phát, mang lại những ứng dụng thực tế cho các ứng dụng xử lý nước thải tiên tiến.

DOI: https://doi.org/10.34238/tnu-jst.12629

Email: nguyentrongnghia@utehy.edu.vn

1. Introduction

Phosphorus is an essential nutrient for biological growth and development, and at low concentrations, it is not classified as harmful or toxic to humans. In aquatic environments, phosphorus primarily exists in the form of dissolved phosphates, including orthophosphates, polyphosphates, and organic phosphates [1], [2]. Among these, orthophosphate is the most thermodynamically stable and prevalent species, accounting for approximately 50% of the total phosphate content [3], [4]. Due to their chemical instability in aqueous media, polyphosphates are prone to hydrolysis, converting into orthophosphates, which are consequently the most commonly detected form in natural waters [5]. Anthropogenic activities, particularly in agriculture and industry, have significantly intensified phosphate loading into the environment. The excessive application of phosphate-based fertilizers and intensified agricultural practices have made agricultural runoff a dominant source of phosphate pollution. Moreover, population growth has led to increased imports of phosphate-rich animal feed and fertilizers, further elevating phosphate concentrations in freshwater systems in developed nations [2], [6], [7]. In parallel, the use of phosphate-containing compounds in fossil fuel combustion, detergents, personal care products, and industrial processes has contributed to rising phosphate levels in municipal and industrial wastewater. Elevated phosphate concentrations in aquatic systems lead to a range of ecological and operational challenges. Concentrations exceeding 100 μg P/L are known to trigger eutrophication, characterized by excessive algal growth, reduced light penetration, impaired gas exchange, and severe oxygen depletion. In industrial settings, phosphate can cause pipe fouling and interfere with the removal of other contaminants, such as arsenate. Additionally, while not acutely toxic, elevated phosphate levels in drinking water are considered a potential health concern. Consequently, the U.S. Environmental Protection Agency (EPA) has established stringent regulatory thresholds: 0.05 mg/L for surface waters discharging into lakes or reservoirs, and 0.1 mg/L for drinking water supplies [8], [9].

To comply with stringent phosphate discharge regulations, a variety of treatment technologies such as adsorption, biodegradation, chemical precipitation, and electrocoagulation have been implemented for phosphate removal from water and wastewater streams [10], [11]. Among these, electrocoagulation (EC) has gained increasing attention as a viable and efficient alternative to conventional treatment methods. EC operates by generating coagulant species in situ through the application of an electric current across metallic electrodes, typically aluminum or iron. This technique is valued for its operational simplicity, ease of automation, rapid treatment times, and effectiveness in removing fine particulate matter [12], [13]. A notable advantage of EC is its minimal chemical input, which reduces the risk of secondary pollution and lowers sludge generation, aligning it with principles of green and sustainable technology. EC has demonstrated high removal efficiencies for a broad spectrum of contaminants, including pathogens, heavy metals, strontium, phosphate, and various organic compounds, often within relatively short treatment durations [5], [12]. However, in conventional electrocoagulation systems, electrode passivation occurs due to the accumulation of insoluble layers on the electrode surfaces, which gradually reduces current efficiency and diminishes contaminant removal performance. Furthermore, the continuous dissolution of the anode during electrolysis necessitates frequent replacement, thereby increasing operational costs. Polarity reversal mode electrocoagulation (PRM-EC) effectively mitigates these limitations by periodically reversing the electrode polarity [14], [15]. This mechanism promotes self-cleaning of the electrode surfaces and prevents the formation of passive oxide layers, ensuring sustained and uniform electrode activity [16]. As a result, the pollutant removal efficiency is enhanced, while maintenance frequency and system downtime are significantly reduced. The more uniform generation of coagulant species in PRM-EC further facilitates the effective removal of pollutants [17].

The present study aims to optimize the removal of phosphate from aqueous solutions using a PRM-EC system equipped with aluminum electrodes. Optimization of the process was carried out using response surface methodology (RSM), with a central composite design (CCD) employed to develop the experimental matrix. The influence of three key operational parameters—current density, electrolysis time, and polarity reversal interval—was systematically investigated to maximize phosphate removal efficiency.

2. Experiment and method

Analytical-grade potassium dihydrogen phosphate (KH_2PO_4), sodium chloride (NaCl), sodium hydroxide (NaOH), and hydrochloric acid (HCl) were used without further purification. High-purity aluminum plates (Al, 99.5%) served as the electrodes in the electrocoagulation (EC) system. The aluminum electrodes, with dimensions of 5.0 cm × 2.5 cm × 0.5 cm, were polished using sandpaper and subsequently cleaned with 5% HCl followed by rinsing with double-distilled water (DDW) to remove surface impurities. The EC setup consisted of a glass reactor containing 1 L of the working solution. The aluminum electrodes were vertically positioned within the reactor and connected to a time-controlled polarity reversal unit, which was linked to a direct current (DC) power supply. Each electrode had an effective immersed surface area of 40 cm². Homogeneity of the reaction medium was ensured using a mechanical stirrer operating at 150 rpm. The initial phosphate concentration in the solution was adjusted to 80 mg/L, with 1% NaCl added as a supporting electrolyte. During electrolysis, 3 mL aliquots were periodically withdrawn, filtered, and analyzed for phosphate concentration. The phosphate content was determined using the ascorbic acid method with a V-770 spectrophotometer (Jasco) at a wavelength of 880 nm.

Phosphate removal efficiency (PPR) was calculated using the following equation:

$$PPR\ (\%) = (C_o - C) \times 100/C_o \quad (1)$$

where C_o is the initial phosphate concentration (mg/L), and C (mg/L) is the phosphate concentration at the sampling time.

To optimize the EC process, response surface methodology (RSM) was employed using a central composite design (CCD). This design included three independent variables: current density (J), electrolysis time (ET), and polarity reversal interval (PRI). Each variable was studied at five levels: low (-1), high (+1), center (0), and two axial points. The actual and coded values for these variables at each level are presented in Table 1.

Table 1. *Actual and coded values of the independent variables at five levels*

Independent variables	Range				
	-α	**-1**	**0**	**+1**	**+α**
J (A/m^2)	16.8	25	37.5	50	58.5
ET (min)	9.8	20	35	50	60.2
PRI (min)	0.32	1	2	3	3.7

3. Results and discussion

3.1. Model selecting

Table 2 presents the results of fitting the experimental data to four different regression models: linear, two-factor interaction (2FI), quadratic, and cubic. Each model was evaluated based on its sequential p-value, lack of fit p-value, adjusted R^2, and predicted R^2 values.

Table 2. *Summary of fitting experimental data to linear, 2FI, quadratic, and cubic models*

Source	Sequential p-value	Lack of Fit p-value	Adjusted R^2	Predicted R^2
Linear	< 0.0001	< 0.0001	0.6913	0.5668
2FI	0.9195	< 0.0001	0.6338	0.4895
Quadratic	**< 0.0001**	**0.1211**	**0.9930**	**0.9772**
Cubic	0.0600	0.5459	0.9969	0.9820

The quadratic model demonstrated the best overall performance in fitting the experimental data. It exhibited a highly significant sequential p-value (< 0.0001), indicating that the model adds substantial value beyond the simpler models. Importantly, the lack of fit p-value for the quadratic model (0.1211) was not significant, suggesting that the model adequately represents the experimental data without over-fitting [18], [19]. The quadratic model also showed high statistical reliability, with an adjusted R^2 of 0.9930 and a predicted R^2 of 0.9772, indicating excellent agreement between observed and predicted responses. In comparison, both the linear and 2FI models had a significant lack of fit and lower R^2 values, suggesting an inadequate representation of the system's behavior. Although the cubic model provided slightly higher R^2 values (adjusted $R^2 = 0.9969$; predicted $R^2 = 0.9820$), its sequential p-value (0.0600) was not statistically significant [20], [21]. Moreover, the cubic model includes more parameters, increasing the risk of over-fitting, particularly in the absence of sufficient degrees of freedom for pure error. Based on these results, the quadratic model was selected as the most appropriate and statistically robust model for describing the phosphate removal process under the given experimental conditions.

3.2. Analysis of variance of the selected model

The statistical significance of the quadratic model and its individual terms was evaluated through analysis of variance (ANOVA), as summarized in Table 3.

Table 3. *ANOVA for quadratic model*

Source	Sum of Squares	df	Mean Square	F-value
Model	2031.78	9	225.75	299.96
A-J	1200.14	1	1200.14	1594.65
B-ET	305.64	1	305.64	406.12
C-PRI	3.34	1	3.34	4.44
AB	10.58	1	10.58	14.06
AC	6.81	1	6.81	9.05
BC	1.81	1	1.81	2.40
A^2	466.67	1	466.67	620.07
B^2	7.68	1	7.68	10.20
C^2	26.91	1	26.91	35.76
Residual	7.53	10	0.7526	
Lack of Fit	5.68	5	1.14	3.08
Pure Error	1.84	5	0.3687	
Cor Total	2039.30	19		

The ANOVA results confirm that the quadratic model is highly significant ($p < 0.0001$), with a very high F-value of 299.96. This indicates that the model effectively captures the variability in phosphate removal and is statistically reliable. Among the linear terms, current density (A–J) and electrolysis time (B–ET) were extremely significant ($p < 0.0001$), demonstrating their strong influence on phosphate removal efficiency. In contrast, the polarity reversal interval (C–PRI) showed a marginal effect ($p = 0.0614$), suggesting a lesser but still notable role. The interaction terms AB (J×ET) and AC (J×PRI) were also statistically significant ($p < 0.05$), indicating synergistic effects between current density and the other two variables. The BC (ET×PRI) interaction, however, was not significant ($p = 0.1525$), suggesting no meaningful combined effect. Regarding the quadratic terms, all three (A^2, B^2, and C^2) were statistically significant ($p < 0.01$), confirming the presence of curvature in the response surface and reinforcing the appropriateness of the quadratic model. The non-significant lack of fit ($p = 0.1211$) further supports the adequacy of the model, indicating that the observed deviations from the experimental data can be attributed to random error rather than model inadequacy. Overall, the ANOVA results validate the use of the quadratic model for accurately predicting phosphate removal and identifying optimal operational parameters in the PRM-EC system. Thus, the

relationship between phosphate percentage removal (response Y) and the three factors (coded values) can be represented by the following equation:

$$\mathrm{PPR} = 90.5 + 9.37\mathrm{A} + 4.73\mathrm{B} - 1.15\mathrm{AB} + 0.922\mathrm{AC} - 5.69\mathrm{A}^2 - 73\mathrm{B}^2 - 01.73C^2, \quad (2)$$

Figure 1 illustrates the parity plot comparing the actual experimental values of phosphate percentage removal with those predicted by the quadratic model. The data points are closely aligned along the 45° reference line, indicating a high degree of agreement between observed and predicted responses. This alignment confirms the robustness and predictive accuracy of the developed model. The minimal deviation from the reference line suggests that the quadratic model effectively captures the underlying relationship between the process variables (current density, electrolysis time, and polarity reversal interval) and the response (PPR). This graphical evidence is consistent with the statistical indicators from the model fitting and ANOVA (Adjusted R^2 = 0.9930; Predicted R^2 = 0.9772), both of which support the model's strong explanatory and predictive power. The absence of systematic error patterns in the plot further affirms that the model does not suffer from bias and is suitable for optimization.

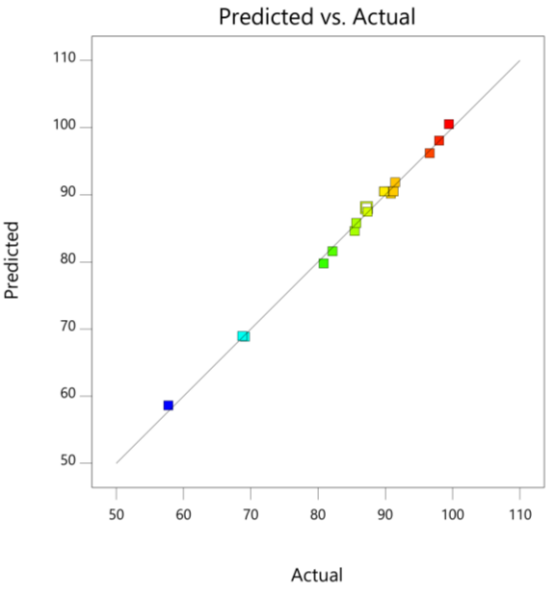

Figure 1. *Predicted value vs. actual value of PPR*

3.3. Three-dimensional response surface plots for phosphate removal

To visualize the interaction effects of operational parameters on phosphate percentage removal, three-dimensional response surface plots were constructed based on the quadratic model. Figure 2 illustrates the combined influence of current density, electrolysis time, and polarity reversal interval on the PPR.

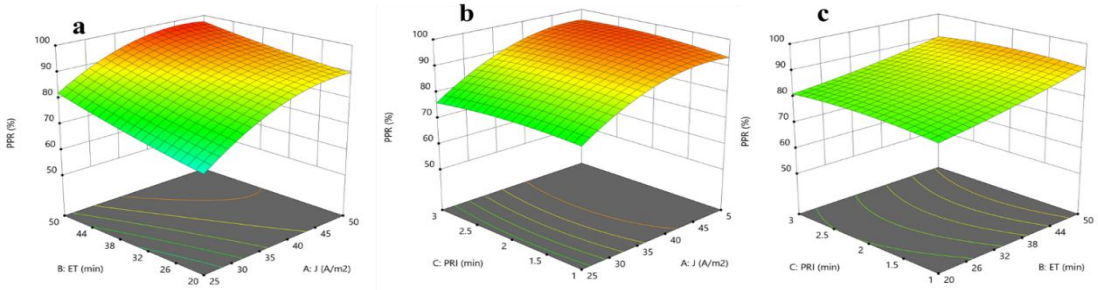

Figure 2. *Three-dimensional response surface plots for phosphate removal*

As presented in Figure 2a, the interaction between current density and electrolysis time reveals a strong synergistic effect. As both variables increase, phosphate removal efficiency significantly improves, reaching values above 90%. This suggests that sufficient reaction time and charge loading are critical for coagulant generation and pollutant destabilization. The surface plot of current density versus polarity reversal interval (Figure 2b) indicates that phosphate removal is predominantly influenced by current density, while PRI shows a minor effect. Nevertheless, slight improvements in removal efficiency can be observed at shorter PRI values, which may help maintain electrode surface activity and reduce passivation. The interaction between electrolysis time and polarity reversal interval shows a relatively flat surface, suggesting minimal interaction.

Phosphate removal efficiency remains high across the range of both variables, implying that once sufficient reaction time is provided, variations in polarity reversal interval do not substantially impact the outcome within the tested range. According to these results, the response surfaces confirm that current density and electrolysis time are the most influential parameters, consistent with the ANOVA results. The plots also demonstrate the suitability of the quadratic model in accurately capturing system behavior across the experimental domain.

3.4. Numerical optimization for the phosphate removal

Numerical optimization techniques were employed to identify the optimal operating conditions for maximizing phosphate percentage removal. The optimization was guided by the response surface methodology, using a desirability function approach. The selection criteria are summarized in Table 4.

Table 4. *Criteria of the parameters for the optimization process*

Name	Goal	Lower Limit	Upper Limit	Lower Weight	Upper Weight	Importance
A: J	is in range	25	50	1	1	3
B: ET	is in range	20	50	1	1	3
C: PRI	is in range	1	3	1	1	3
PPR	maximize	57.7	99.4	1	1	5

The optimal conditions identified were a current density of 46.8 A/m² and an electrolysis time of 50 minutes, with a polarity reversal interval of 2.26 minutes. The associated desirability score of 0.99 indicates excellent agreement between the predictive model and the targeted response, reflecting high reliability in the model's predictive capability. Under these optimized conditions, the model predicted a phosphate removal efficiency of 99.02%. To experimentally validate the optimized parameters, three experiments were conducted under the proposed optimal conditions. The observed PPR values were 98.64%, 99.25%, and 98.75%, yielding an average removal efficiency of 98.91%. These results are in close agreement with the model prediction, with minimal deviation, thereby confirming the accuracy and robustness of the quadratic model for optimizing phosphate removal using the polarity reversal mode electrocoagulation system.

4. Conclusion

This study demonstrated the effectiveness of a polarity reversal mode electrocoagulation (PRM-EC) system equipped with aluminum electrodes for the removal of phosphate from aqueous solutions. Process optimization was successfully achieved using response surface methodology based on a central composite design, allowing for a detailed analysis of the effects and interactions of key operational parameters: current density, electrolysis time, and polarity reversal interval. The statistical analysis confirmed that the quadratic model provided an excellent fit to the experimental data, with high adjusted and predicted R^2 values (0.9930 and 0.9772, respectively) and an insignificant lack of fit ($p = 0.1211$). Current density and electrolysis time were identified as the most influential factors in phosphate removal efficiency, while polarity reversal interval had a less pronounced but supportive role. The maximum phosphate removal (predicted at 99.02%) could be achieved under the following conditions: current density of 46.8 A/m², electrolysis time of 50 minutes, and polarity of 2.26 minutes. Experimental validation closely matched the predicted results, confirming the reliability and robustness of the model. The polarity reversal mode electrocoagulation system proved to be a highly effective, environmentally friendly, and controllable technique for phosphate removal, offering minimal chemical input and sludge production.

REFERENCES

[1] A. Attour, M. Touati, M. Tlili, M. Ben Amor, F. Lapicque, and J. P. Leclerc, “Influence of operating parameters on phosphate removal from water by electrocoagulation using aluminum electrodes,” *Sep. Purif.*

Technol., vol. 123, pp. 124–129, 2014, doi: 10.1016/j.seppur.2013.12.030.
[2] Y. Tian, W. He, X. Zhu, W. Yang, N. Ren, and B. E. Logan, "Improved Electrocoagulation Reactor for Rapid Removal of Phosphate from Wastewater," *ACS Sustain. Chem. Eng.*, vol. 5, no. 1, pp. 67–71, 2017, doi: 10.1021/acssuschemeng.6b01613.
[3] W. Fu *et al.*, "Design optimization of bimetal-modified biochar for enhanced phosphate removal performance in livestock wastewater using machine learning," *Bioresour. Technol.*, vol. 418, p. 131898, 2025.
[4] V. Kuokkanen, T. Kuokkanen, J. Rämö, U. Lassi, and J. Roininen, "Removal of phosphate from wastewaters for further utilization using electrocoagulation with hybrid electrodes - Techno-economic studies," *J. Water Process Eng.*, vol. 8, pp. e50–e57, 2015, doi: 10.1016/j.jwpe.2014.11.008.
[5] Q. Hu, L. He, R. Lan, C. Feng, and X. Pei, "Recent advances in phosphate removal from municipal wastewater by electrocoagulation process: A review," *Sep. Purif. Technol.*, vol. 308, no. October 2022, p. 122944, 2023, doi: 10.1016/j.seppur.2022.122944.
[6] J. Qian, X. Zhou, Q. Cai, J. Zhao, and X. Huang, "The Study of Optimal Adsorption Conditions of Phosphate on Fe-Modified Biochar by Response Surface Methodology," *Molecules*, vol. 28, no. 5, 2023, doi: 10.3390/molecules28052323.
[7] A. Dura and C. B. Breslin, "The removal of phosphates using electrocoagulation with Al−Mg anodes," *J. Electroanal. Chem.*, vol. 846, no. January, p. 113161, 2019, doi: 10.1016/j.jelechem.2019.05.043.
[8] E. Lacasa, P. Canizares, C. Saez, F. J. Fernandez, and M. A. Rodrigo, "Electrochemical phosphates removal using iron and aluminium electrodes," *Chem. Eng. J.*, vol. 172, no. 1, pp. 137–143, 2011.
[9] A. Violante, M. Pucci, V. Cozzolino, J. Zhu, and M. Pigna, "Sorption/desorption of arsenate on/from Mg-Al layered double hydroxides: Influence of phosphate," *J. Colloid Interface Sci.*, vol. 333, no. 1, pp. 63–70, 2009, doi: 10.1016/j.jcis.2009.01.004.
[10] E. K. Maher *et al.*, "Analysis of operational parameters, reactor kinetics, and floc characterization for the removal of estrogens via electrocoagulation," *Chemosphere*, vol. 220, pp. 1141–1149, 2019, doi: 10.1016/j.chemosphere.2018.12.161.
[11] A. Dura and C. B. Breslin, "Electrocoagulation using stainless steel anodes: Simultaneous removal of phosphates, Orange II and zinc ions," *J. Hazard. Mater.*, vol. 374, no. April, pp. 152–158, 2019, doi: 10.1016/j.jhazmat.2019.04.032.
[12] Y. Yang *et al.*, "Removal of phosphate in secondary effluent from municipal wastewater treatment plant by iron and aluminum electrocoagulation: Efficiency and mechanism," *Sep. Purif. Technol.*, vol. 286, 2022, Art. no. 120439, doi: 10.1016/j.seppur.2021.120439.
[13] S. Zhang, J. Zhang, W. Wang, F. Li, and X. Cheng, "Removal of phosphate from landscape water using an electrocoagulation process powered directly by photovoltaic solar modules," *Sol. Energy Mater. Sol. Cells*, vol. 117, pp. 73–80, 2013, doi: 10.1016/j.solmat.2013.05.027.
[14] H. Zhao, J. Chang, A. Boika, and A. J. Bard, "Electrochemistry of high concentration copper chloride complexes," *Anal. Chem.*, vol. 85, no. 16, pp. 7696–7703, 2013, doi: 10.1021/ac4016769.
[15] A. Almukdad, M. A. Hafiz, A. T. Yasir, R. Alfahel, and A. H. Hawari, "Unlocking the application potential of electrocoagulation process through hybrid processes," *J. Water Process Eng.*, vol. 40, no. February, p. 101956, 2021, doi: 10.1016/j.jwpe.2021.101956.
[16] M. Mahmood, N. G. Yasri, and E. P. L. Roberts, "Electrocoagulation Using a Hybrid Combination of Iron and Aluminum Electrodes with Asymmetric Polarity Reversal," *ACS ES T Water*, vol. 5, no. 2, pp. 703–712, 2025, doi: 10.1021/acsestwater.4c00762.
[17] J. N. Hakizimana *et al.*, "Electrocoagulation process in water treatment: A review of electrocoagulation modeling approaches," *Desalination*, vol. 404, pp. 1–21, 2017, doi: 10.1016/j.desal.2016.10.011.
[18] M. A. Bezerra, R. E. Santelli, E. P. Oliveira, L. S. Villar, and L. A. Escaleira, "Response surface methodology (RSM) as a tool for optimization in analytical chemistry," *Talanta*, vol. 76, no. 5, pp. 965–977, 2008, doi: 10.1016/j.talanta.2008.05.019.
[19] J. P. C. Kleijnen, "Response surface methodology," *Int. Ser. Oper. Res. Manag. Sci.*, vol. 216, no. 2, pp. 81–104, 2015, doi: 10.1007/978-1-4939-1384-8_4.
[20] G. I. Danmaliki, T. A. Saleh, and A. A. Shamsuddeen, "Response surface methodology optimization of adsorptive desulfurization on nickel/activated carbon," *Chem. Eng. J.*, vol. 313, pp. 993–1003, 2017, doi: 10.1016/j.cej.2016.10.141.
[21] M. S. Bhatti, A. S. Reddy, R. K. Kalia, and A. K. Thukral, "Modeling and optimization of voltage and treatment time for electrocoagulation removal of hexavalent chromium," *Desalination*, vol. 269, no. 1–3, pp. 157–162, 2011, doi: 10.1016/j.desal.2010.10.055.